Embryonic PCB exposure alters phenotypic, genetic, and epigenetic profiles in turtle sex determination, a biomarker of environmental contamination

Yuiko Matsumoto, Brette Hannigan, David Crews

Department of Integrative Biology, University of Texas at Austin, 2415 Speedway St., Austin, TX 78712, USA.

In species with temperature-dependent sex determination or TSD, embryonic gonadal differentiation can be modified by an exposure to exogenous chemicals such as environmental contaminants. Although phenotypic outcomes of such event are well documented, the underlying molecular mechanisms are rarely described. Here we examine the genetic and epigenetic effect of the embryonic exposure to polychlorinated biphenyls (PCBs) on gonad differentiation in red-eared slider turtles (*Trachemys scripta*). Some PCB congeners are without effect, while others synergize to alter sex determination in this species. Application of two potent PCB congeners alter the physiological processes of gonad development normally dictated by the male-producing temperature (MPT), resulting sex ratios significantly biased towards female hatchlings. Of these PCB-induced females, oviduct formation is prominently distorted regardless of ovary development. Further, gonadal expression of ovarian markers, *aromatase*, *FoxL2*, and *Rspo1,* is activated while testicular markers, *Dmrt1* and *Sox9,* is suppressed compared to typical expression patterns observed at MPT. DNA methylation profiles of the aromatase promoter in PCB-treated gonads do not follow the typical methylation pattern observed in embryos incubating at female-producing temperature (FPT) rather the MPT-typical methylation profiles is retained in spite of the induced ovarian formation. Overall, our studies demonstrate that PCB exposure alters the transcriptional profiles of genes responsible for gonadal differentiation, but does not re-establish the epigenetic marks of the aromatase promoter normally set by incubation temperatures in embryonic gonads.

Endocrine disrupting compounds (EDCs) are chemicals in the environment that interfere with normal endocrine functions of organisms. Industrial use of polychlorinated biphenyls (PCBs) has been banned in the United States since the late 1970's but, due to their long half-life and chemical inability to oxidize in nature, residual contamination will persist in the environment for centuries (1–3). PCBs bioaccumulate in fatty tissue of organisms throughout the food web and tertiary consumers, including humans, are particularly vulnerable (4–6). Early life exposure to EDCs, particularly during sex determination, can result in subor infertility and, in some cases, complete sex reversal (7–10).

In the red-eared slider turtle (*Trachemys scripta*), the resulting sex of the embryonic gonad depends on the ambient temperature in which the egg is incubated, a system known as temperature-dependent sex determination (TSD). During the temperature-sensitive period (TSP) of development, embryonic gonads are also sensitive to exogenous steroid hormones and hormone mimics. Exposure to exogenous EDCs, including some PCBs, redirects the gonadal trajectory from that normally dictated by incubation temperature (7, 11–13). The plasticity of sexual development in species with TSD makes them an excellent model system to study the interaction of environmental and molecular mechanism during embryonic development. Therefore species with TSD are often considered as a biomarker of environmental contamination.

This study focuses on the molecular mechanisms underlying EDC-directed gonad determination. Previous re-

ISSN Print 0013-7227 ISSN Online 1945-7170
Printed in U.S.A.

Received May 20, 2014. Accepted August 1, 2014.

Abbreviations: TSD, Temperature-dependent sex determination; FPT, Female-producing temperature; MPT, Male-producing temperature; TSP, Temperature-sensitive period

search demonstrates that temperature- as well as hormone-induced changes in gonad phenotypes are accompanied by developmental changes in the expression of candidate sex determining genes (14–16). It suggests that the transcriptional activation or repression of these genes may be the key mechanism determining the trajectory of the developing gonad. Here the effect of PCB treatment on the expression of candidate sex-determining genes was examined in developing gonads of slider turtles: *cyp19a1* (*aromatase*), *Fork-head box protein L2* (*FoxL2*), *R-spondin 1* (*Rspo1*) as ovarian markers; *Doublesex mab3- related transcription factor 1* (*Dmrt1*) and *sex-determining region on Y chromosome-box 9* (*Sox9*) as testicular markers. Further, we examined the epigenetic status of one of the candidate genes, aromatase to assess the potential target of EDCs during gonad differentiation. Aromatase catalyzes conversion of androgens into estrogens and is pivotal in TSD (12, 17, 18). The aromatase promoter is one of the targets of DNA methylation during gonad determination and the methylation pattern strongly correlates with the gonad-specific expression of aromatase in both genetic and environmental sex-determination systems (19–22). The current study focused on the DNA methylation profiles of the aromatase promoter during the beginning and middle of the TSP, the period when temperature establishes the developmental trajectory of the gonad.

Materials and Methods

Animals and treatment groups

Freshly laid slider turtle eggs were collected within 24 hours of laying and shipped from Kliebert's Turtle and Alligator Farm in Hammond, LA. All embryos were maintained and handled in accordance with humane animal practices under IACUC protocol number AUP-00149. Eggs were maintained at room temperature (approximately 26°C) for 10 days before viability was assessed by candling. Viable eggs were randomly placed in trays with moistened vermiculite and incubated at either 26°C (= male-producing temperature or MPT) for subsequent PCB treatments or 31°C (= female-producing temperature or FPT) to serve as normal ovarian development (FPT control). Incubation temperature was monitored by thermometers and HOBO data loggers (Onset Computer Corp., Bourne, MA). Embryonic development was determined by morphological features according to the Greenbaum's staging series (23).

PCB treatment and gonad collection

Two types of PCBs, 4-hydroxy-2′,4′,6′-trichlorobiphenyl (PCB-F) and 4-hydroxy-2′,3′,4′,5′-tetrachlorobiphenyl (PCB-G) (AccuStandard, New Haven, CT) were chosen based on previous research regarding their effect on hatchling sex ratio when topically applied to eggs during the development of slider turtles (7). At stage 16, the beginning of TSP when all embryonic gonads are sensitive to surrounding temperature and exogenous hormones, MPT incubated eggs were treated with one dose of (i) 10 μL ethanol (EtOH) as a vehicle control, (ii) 10 μg 17β-estradiol (E_2, Sigma-Aldrich, MO) as a positive hormone control, (iii) 100 μg PCB-F (= low PCB-F), (iv) 200 μg PCB-F (= high PCB-F), (v) 100 μg PCB-G (= low PCB-G), (vi) 200 μg PCB-G (= high PCB-G), or (vii) 100 μg each of PCB-F&G (= mixture) and kept at MPT. As a control for the natural ovarian gonadal pathway, FPT incubated eggs also received 10 μL EtOH vehicle at the same time point, stage 16 and were kept at FPT. For the baseline assessment, the gonads at stage 16 (n = 8–10 gonads, 1 gonad per sample) at both temperatures were taken before the treatments, collected individually in 500 μl Trizol reagent (Life Technologies, Grand Island, NY), vortexed, and stored at –80°C until use. This time point would represent baseline gene expression for both *in ovo* and in vitro (see Supplemental Figure 2) experiments. Three treatment groups - E_2, high PCB-F, and a mixture of PCB-F&G - were selected for subsequent gene expression and DNA methylation analysis due to robust effect on hatchling sex ratio observed in this study (Figure 1) along with EtOH vehicle controls at both temperatures. Six to eight individual gonads (1 gonad per sample) in each treatment group were separately collected in 500 μl Trizol reagent at stage 17, 19, 23, and hatching, vortexed, and stored at –80°C until RNA extraction. For DNA methylation analysis, gonads from 6 to 8 individual embryos (2 gonads per sample) at stage 16, 17, and 19 were collected and snap frozen in liquid nitrogen until bisulfite conversion. The gonads from four individuals (2 gonads per sample) from MPT eggs without any treatment were also collected at each stage to assure the absence of any influence of the EtOH vehicle on DNA methylation, which has not been reported in previous studies.

Gonad sex determination by microscopy

At hatching, the hatchling's sex was determined by phenotypic features of the gonads under the microscope and recorded by two independent investigators. All treatments were coded in a double blind manner to the investigators to prevent observational prejudice. Male was evidenced by the formation of vascularized and round testes, whereas female was evidenced by the formation of nonvascularized elongated ovaries (24, 25). A presence or absence of the oviducts was also recorded but not taken into consideration in the determination of the individual's sex. A whole adrenal-kidney-gonad (AKG) complex from several individuals per each treatment was preserved in 70% EtOH and photographed using Zeiss SteREO Discovery V12 (Zeiss, Thornwood, NY).

RNA extraction and quantitative PCR

Total RNA was isolated, treated with DNA-Free Turbo DNase I (Life Technologies), and reverse transcribed using iScript kit (Bio-Rad, Hercules, CA) as previously described (16). Relative gene expression was examined by quantitative PCR (qPCR) using SYBR green real-time PCR master mix (Life Technologies) on the ViiA7 System (Life Technologies). Samples were run in triplicate, and the median Ct value was used for analysis. The expression of *aromatase*, *FoxL2*, *Rspo1*, *Sox9*, and *Dmrt1* were examined using previously published primers (15, 26, 27). The expression of protein phosphatase1 (PP1) was used as an internal control to normalize Ct values of all genes (27). Samples with PP1 Ct values of more than 35 were considered degraded or

with insufficient amounts of RNA and therefore removed from the analysis. PCR specificity was monitored using melting curve analysis. Ct values were analyzed using the ΔCT method and fold changes of the treatment groups to their respective control was calculated by setting the sample with the lowest Ct value as one fold.

Bisulfite conversion and pyrosequencing

Gonads were treated with Proteinase K and bisulfite using EZ DNA Methylation-Direct kit (Zymo research, Irvine, CA) according to the manufacturer's protocol. The bisulfite-treated genomic DNA was purified using columns provided with the kit. Three primer sets, Arom-set1, Arom-set2, and Arom-set3 (Table 1) were designed using PyroMark Assay Design Software (Qiagen, Venlo, Limburg) to capture five CpG sites within the previously identified slider aromatase promoter (21). PCR was carried out using Advantage 2 polymerase mix (Clontech, Mountain View, CA) for Arom-set1 outer and nested primer sets and KAPA HiFi hotstart uracil+ ready mix (KAPA Biosystems, Wilmington, MA) for the Arom-set2 and 3 primer sets. PCR conditions for Arom-set1 outer primers were as follows: 1 minute at 95°C; 32 cycles of 30 seconds at 95°C, 1 minute at 60°C, 1 minute at 68°C; and 10 minutes at 68°C. PCR products were diluted 1:50 with nuclease-free water, and 1 μL of the dilution was used for the subsequent nested PCR reaction using Arom-set1 nested primers under the same PCR conditions as outer PCR reaction with 47 cycles. PCR condition for Arom-set2 and 3 primers were as follows: 3 minutes at 95°C; 47 cycles of 20 seconds at 98°C, 30 seconds at 60°C, 1 minute at 68°C; and 3 minutes at 68°C. The specificity of the PCR reaction was confirmed by the presence of a single band on a 2% agarose gel. PCR products were then sent to EpigenDx (Hopkinton, MA) along with sequence primers (Table 1) for pyrosequencing analysis. Raw data were analyzed and reported as a fraction of C (methylated) or T (unmethylated) at each CpG site by EpigenDx. Only samples that passed a quality assessment by EpigenDx were used for further analysis.

Statistical analysis

Gonad sex ratio was analyzed with the Fisher's exact test. For qPCR and pyrosequencing data, the Wilcoxon Sum test was used to evaluate the differences of EtOH treatment at FPT or exogenous chemical treatments at MPT to the EtOH control at MPT. The same statistical analysis was also used to ensure the absence of EtOH vehicle control effect. A p-value of less than 0.05 was considered to be statistically significant. All statistical analysis and graphic visualizations were conducted using R (The R project for Statistical Computing, Vienna, Austria).

Results

Embryonic exposure to PCBs altered hatching sex ratio biased to females and disrupted development of sex cords

We first examined the sex ratio at hatching from eggs treated with exogenous chemicals. As shown in Figure 1A, topical treatment of E_2 at stage 16 resulted in the expected 100% sex reversal in ambient temperature MPT, producing only females (Fisher's Exact Test, $P < .001$). In this group, we found that approximately 74% of individuals had one or both oviducts missing. The PCB-F and PCB-F & G mixture treatments had significant changes in sex ratio compared to the control (Fisher's Exact Test, $P < .001$), following the findings in the previous report of sliders (7). In these PCB treatment groups, the absence of one

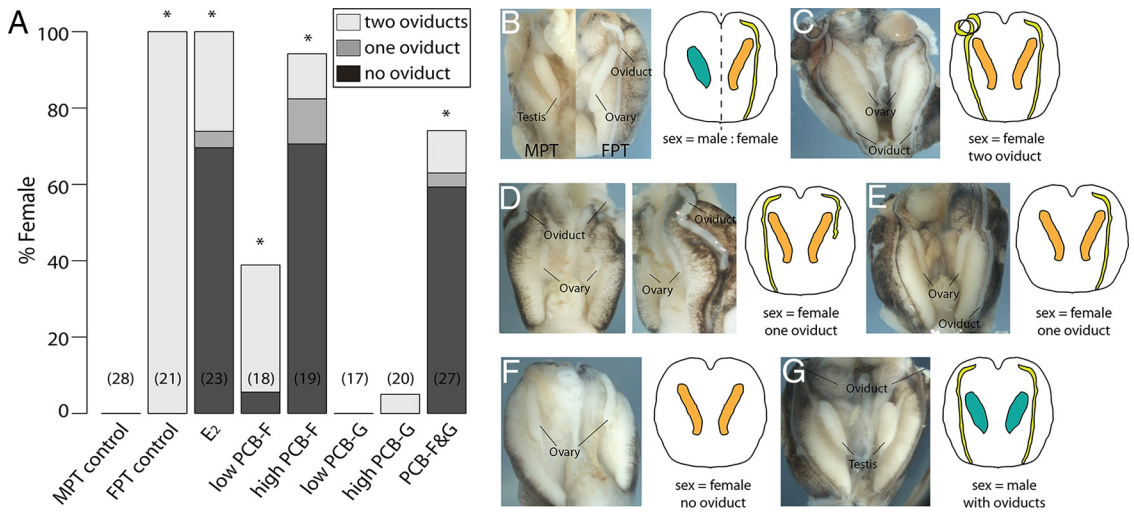

Figure 1. Effects of temperature, exogenous estradiol, and PCBs on hatching sex ratio (A) and phenotypes of adrenal-kidney-gonad (AKG) complex and oviducts (B-G) in the red-eared slider turtle. A, Percent of female hatchings in MPT and FPT control groups, and exogenous chemical treated groups at MPT. Hatchling sex was determined by morphological characteristics of gonads. Sample size for each group is shown in parentheses. Asterisks indicate statistically significant differences from MPT control ($P < .001$, Fisher's exact test). Examples of sex diagnosis and counting the oviduct numbers are indicated in the text below the cartoon figures in B-G. B, Left and right panels are a control testis at MPT and ovary at FPT, respectively. AKG with malformation of reproductive tracts are shown in high PCB-G (C), E_2 (D), PCB-F&G (E), E_2 (F), and low PCB-F (G) treated individuals. E_2 = 10 μg17β-estradiol. Low and high PCB-F = 100 μg and 200 μg 4-hydroxy-2′,4′,6′-trichlorobiphenyl. Low and high PCB-G respectively = 100 μg and 200 μg 4-hydroxy-2′,3′,4′,5′-tetrachlorobiphenyl. PCB-F&G = a mixture of 100 μg each of PCB-F&G.

Table 1. PCR and sequence primers for pyrosequence analysis. Parenthesis represents a direction of primer. F = forward, R = reverse, +b = biotin labeled.

Primer name (direction)	Target CpG	Sequence (5′-3′)
Arom set 1 PCR outer (F)	CpG 1	AGTAGGGATTAGTAAGGAATTTT
Arom set 1 PCR outer (R)	CpG 1	TATTACCCTTAACTAACCAACAA
Arom set 1 PCR nested (F)	CpG 1	TAGTATGGTTGTTTGTTTATG
Arom set 1 PCR nested (R) +b	CpG 1	TATTTTCCCTCCATATCACT
Arom set 1 sequence (F)	CpG 1	AAGTGTTAGATAAAAATAAAGTATA
Arom set 2 PCR (F)	CpG 2, 3	GTGATATGGAGGGAAAATAAG
Arom set 2 PCR (R) +b	CpG 2, 3	TAAAACTCAAATTCCTTTAAATAC
Arom set 2 sequence (F)	CpG 2, 3	AGAGTTTAATTTTTTTTATTATGG[b]
Arom set 3 PCR (F)	CpG 4, 5	GGTAATATTAAAGATAAAAGGTTTATTG
Arom set 3 PCR (R) +b	CpG 4, 5	AACCCCTTTACAAATCCTATA[b]
Arom set 3 sequence 1 (F)	CpG 4	AATGTTTTGTTATTTTTGGG[b]
Arom set 3 sequence 2 (F)	CpG 5	AGTTTGTCTTGTTTAAGTAG[b]

or both oviducts was also prominent. PCB-G alone did not have a significant effect on sex reversal, although a higher dose of PCB-G produced slightly more female hatchings than the lower dose. We next examined by microscopy the phenotype of the adrenal-kidney-gonad (AKG) complex along with the sex cords at hatching. Hatchlings at MPT exhibited the typical phenotype of sex organs in this species, comprised of round, vascularized testes with degenerating or degenerated oviducts (Figure 1B, left panel). Hatchlings at FPT exhibited typical elongated nonvascularized ovaries along with oviducts formed vertically on the mesonephros tissue (Figure 1B, right panel). AKG complexes from eggs treated with exogenous chemicals, E_2 or PCBs at MPT showed ovaries with several malformations of the oviducts such as enlarged (Figure 1C), incompletely elongated (Figure 1D), or missing (Figure 1, E and F) oviducts. A small group of females in the E_2 treatment group had smaller ovaries compared to the FPT controls, as previously reported in turtles (25, 28, 29). No prominent phenotypic changes were observed in PCB-induced ovaries. Some (~ 7%) males in the treatment groups exhibited testes development with a failure of oviduct degeneration (Figure 1G). The effects of E_2 or PCB exposure to embryos on hatching sex ratio and phenotypes of AKGs were also examined at FPT. The four treatments, E_2, high PCB-F, high PCB-G, or a mixture of PCB-F&G were tested under the same condition described above, except eggs were incubated at FPT before and after the treatment. As expected, all hatchlings were females in all treatment groups (Supplemental Figure 1A). We found some individuals also had oviduct malformations; however fewer incidences were observed than in those incubated at MPT (Supplemental Figure 1, A for percentage and B-F for phenotype).

The expression of candidate sex-determining genes was altered in PCB-treated gonads

We proceeded to analyze the *in ovo* expression of candidate sex-determining genes in the three treatment groups that showed the most significant effects on hatchling ratio, ie, E_2, high PCB-F, and a mixture of PCB-F&G along with control groups. Two control groups, MPT and FPT incubated eggs roughly followed our previous findings (15, 16, 26, 27) of up-regulation of ovarian markers and down-regulation of testicular markers at FPT and vice versa at MPT (Figure 2A) although the timing of the expression peaks in ovarian markers were slightly different from previous studies (see Discussion). When the pattern of gonadal gene expression during development in each treatment group was compared to the MPT control group, we found PCB-treated gonads exhibited a similar expression pattern to the gonads treated with E_2. The expression of *aromatase,* typically suppressed at MPT, increased as early as stage 19 in E_2 and PCB treatment groups (Figure 2B). Another ovarian marker, *FoxL2* rapidly increased in both groups of PCB treatments as well as the E_2 positive control group. *Rspo1* did not increase until stage 23 in E_2 and PCB treatments. In all ovarian markers tested, the responses in gene expression were prominent particularly in E_2 and high PCB-F treatment groups, which also corresponded with the higher percentage of female hatchings in these groups (Figure 1A). The increase of these markers in treatment groups, however, occurred at later developmental stages than observed in normal ovarian development at FPT (Figure 2B compared to Figure 2A). The expression of testicular markers *Dmrt1* and *Sox9* were significantly suppressed by E_2 and high PCB-F treatment at all developmental time points (Figure 2B). Unlike ovarian markers, testicular markers were suppressed by exogenous chemicals with similar pattern and timing as ob-

served in ovarian pathway control at FPT (Figure 2B compared to Figure 2A). We also examined PCBs effect on candidate sex-determining genes in vitro. Previous studies showed that the expression pattern of candidate sex-determining genes after exogenous ligand treatment (steroid hormones and an inhibitor for the steroid metabolic enzyme) in an in vitro gonad culture mimicked the gonadal gene expression pattern *in ovo* (16). In this study, we chose two genes; *FoxL2* as an ovarian marker and *Dmrt1* as a testicular marker, due to limited amount of total RNA available for testing. These two genes were chosen because of their rapid transcriptional responses to the ambient temperatures or exogenous ligands observed *in ovo* (Figure 2). The expression of *FoxL2* increased at day (D) 4 and D12 in E_2 treated gonads, at D1, D4, and D12 in PCB-F treated gonads, and at D1 and D4 in PCB-F&G treated gonads compared to the EtOH control at MPT (Supplemental Figure 2, A and B). The expression of *Dmrt1* was

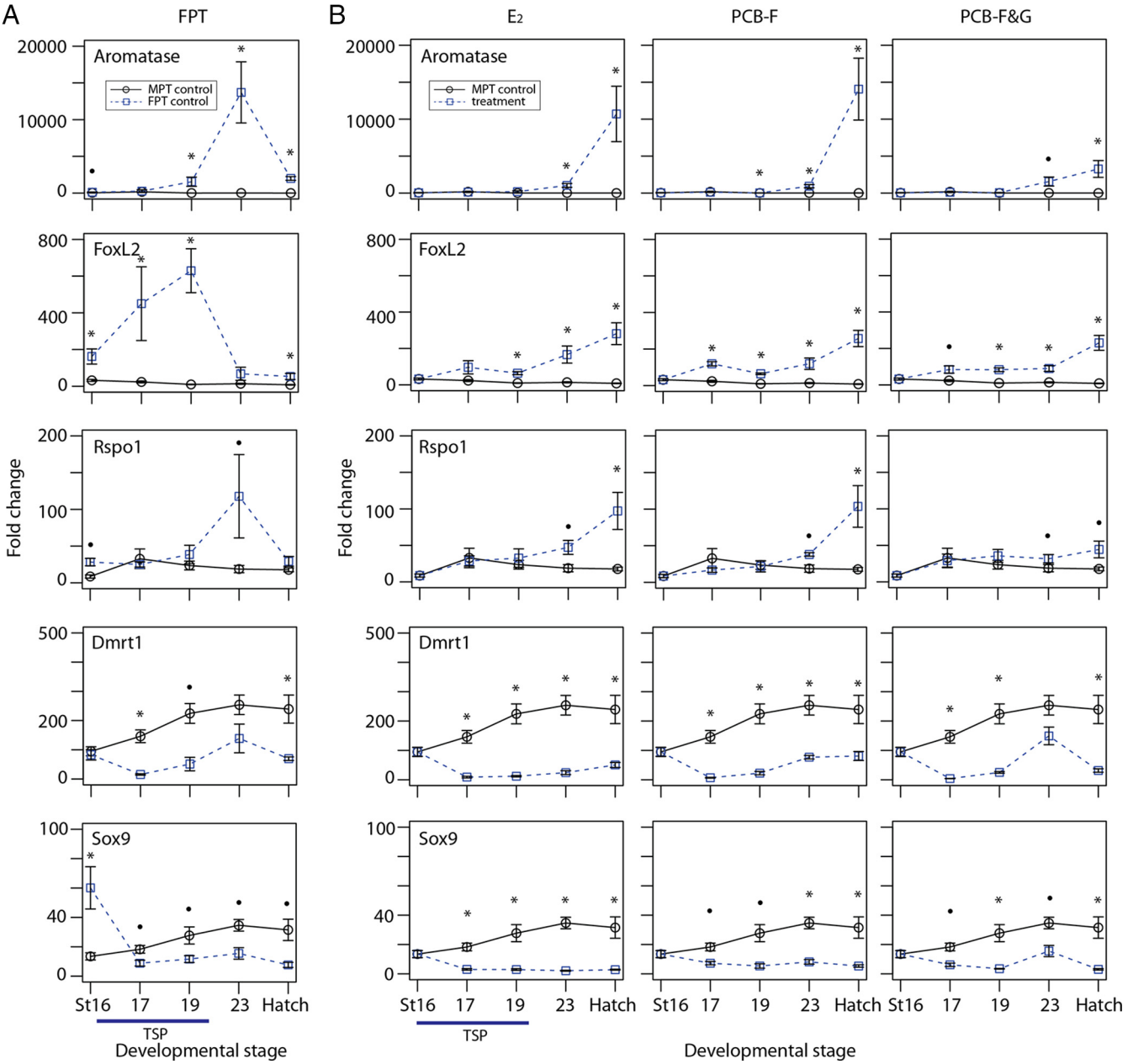

Figure 2. Gonadal expression of candidate sex-determining genes *aromatase*, *FoxL2*, *Rspo1*, *Dmrt1*, and *Sox9* during development *in ovo*. Gene expression in eggs treated with (A) EtOH vehicle at the female-producing temperature (= FPT control) and (B) either E_2, or polychlorinated biphenyls (PCBs) at the male-producing temperature (MPT) are compared to the expression with EtOH vehicle at MPT (= MPT control). Each time point includes n = 6–8 gonads. Data are represented as the mean ± SEM. Significant fold changes compared to the MPT control are indicated with a black circle ($P < .05$) or an asterisk ($P < .001$, Wilcoxon rank sum test). E_2 =10 μg 17β-estradiol. PCB-F = 200 μg 4-hydroxy-2′,4′,6′-trichlorobiphenyl. PCB-F&G = a mixture of 100 μg each of 4-hydroxy-2′,4′,6′-trichlorobiphenyl and 4-hydroxy-2′,3′,4′,5′-tetrachlorobiphenyl. St = stage. TSP = temperature-sensitive period.

suppressed by D4 in E_2- and both PCB-treated gonads. The effect of exogenous chemicals disappeared by D20 in all treatments for *FoxL2* and in the PCB-F treatment for *Dmrt1* expression (Supplemental Figure 2, A and B).

Gonadal DNA methylation of the aromatase promoter sustained MPT-typical profiles in response to embryonic exposure to PCBs

We next examined the DNA methylation status in the aromatase promoter region in the gonads. This region was previously identified as having a differential DNA methylation pattern between the two constant incubation temperatures (21). In the current study, we took advantage of pyrosequencing to obtain deep quantitative sequence reads instead of traditional Sanger sequencing. The percent of successful pyrosequencing analysis at five CpG sites within the aromatase promoter region, CpG 1, 2, 3, 4, and 5 were 90, 100, 100, 78, and 97%, respectively. The difficulty in sequencing at CpG 4 (78%) was most likely attributed to the presence of unidentified mutations unique to individuals rather than technical issues during the procedure. We also discovered some individuals had a three-nucleotide deletion within Arom-set3 sequence primer 1 (data not shown), which necessitated the use of a second sequencing primer, Arom-set3 sequence primer 2 (Table 1) to sequence the CpG 5 position. First, the overall methylation level of the aromatase promoter region containing five CpG sites in each treatment group (including FPT control) was compared to the MPT control within a developmental stage. At stage 19, the FPT control group exhibited a significant decrease of methylation as compared to the MPT control (see an asterisk in Figure 3). Next a change of the methylation level across the developmental stages was examined in each group. We found that the FPT control showed a development-dependent decrease of methylation level (see black dots for statistical differences in Figure 3). Interestingly, the total methylation of E_2 or PCB treated groups followed the methylation pattern observed at MPT rather than at FPT.

Next, we examined the DNA methylation status of individual CpG sites (CpG 1–5, Figure 4A) in the aromatase promoter region. First, each treatment group (including FPT control) was compared to MPT control within a developmental stage. The methylation level in FPT control group was lower than the MPT group in the beginning of TSP, stage 16 at CpG 4, and the pattern found at all CpG sites by stage 19 (Wilcoxon Rank Sum test, Figure 4B). E_2 or PCB-treated groups showed no change or increased level of methylation at CpG 1, 3, 4, and decreased level at CpG 2 (Figure 4B). At CpG 5, the methylation level in E_2 and PCB-F treatments were low at stage 17 and high at stage 19 compared to the MPT control (Figure 4B). Overall, the methylation profiles in E_2 and PCB- treated gonads followed the pattern of those at MPT, although these treatment groups produced most female hatchlings. The FPT-specific decrease of DNA methylation level across stages was commonly observed in all CpG sites (Figure 4B, see Supplemental Table 1 for p-values).

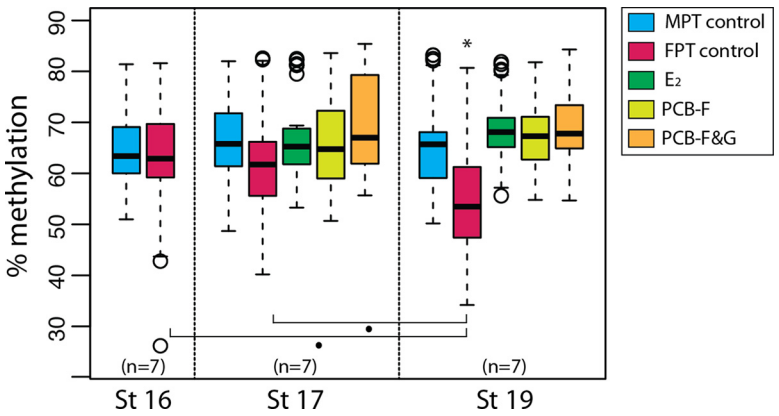

Figure 3. Total percent of DNA methylation of five CpG sites in the gonadal aromatase promoter as detected by pyrosequencing during temperature-sensitive period. Box plot indicates interquartile range (IQR) and median. A dotted line indicates the data range with maximum 1.5 IQR. Outliers are indicated with open circles. Statistical differences across stages in control groups are indicated with black dots ($P < .01$, Wilcoxon rank sum test) and the difference as compared to the MPT control within a stage in both control and treatment groups are indicated with asterisks ($P < .05$, Wilcoxon rank sum test). MPT control = EtOH vehicle at male-producing temperature. FPT control = EtOH vehicle at female-producing temperature. E_2 =10 μg 17β-estradiol. PCB-F = 200 μg 4-hydroxy-2′,4′,6′-trichlorobiphenyl. PCB-F&G = a mixture of 100 μg each of 4-hydroxy-2′,4′,6′-trichlorobiphenyl and 4-hydroxy-2′,3′,4′,5′-tetrachlorobiphenyl. St = stage

Discussion

This study focused on the effects of PCB exposure to embryonic development in the red-eared slider turtles, a species with TSD. The observations of gonad phenotypes in PCB-treated hatchlings replicate those of Bergeron et al (1994) and extend this work to understand the transcriptional and epigenetic mechanisms during gonadogenesis. Our findings indicate that the embryonic exposure to specific PCBs both redirects the gonadal trajectory against the ambient egg incubation temperature and produces a subset of individuals with malformations of the reproductive tracts. Similar phenomena have been reported in female quails where embryonic exposure to the environmental chemicals results in a short-

ening of the oviducts regardless of fairly normal ovarian development (30, 31). As the regression of the Mullerian duct is regulated by mullerian inhibiting substance (MIS) produced from embryonic testes (32–35), a possible PCB

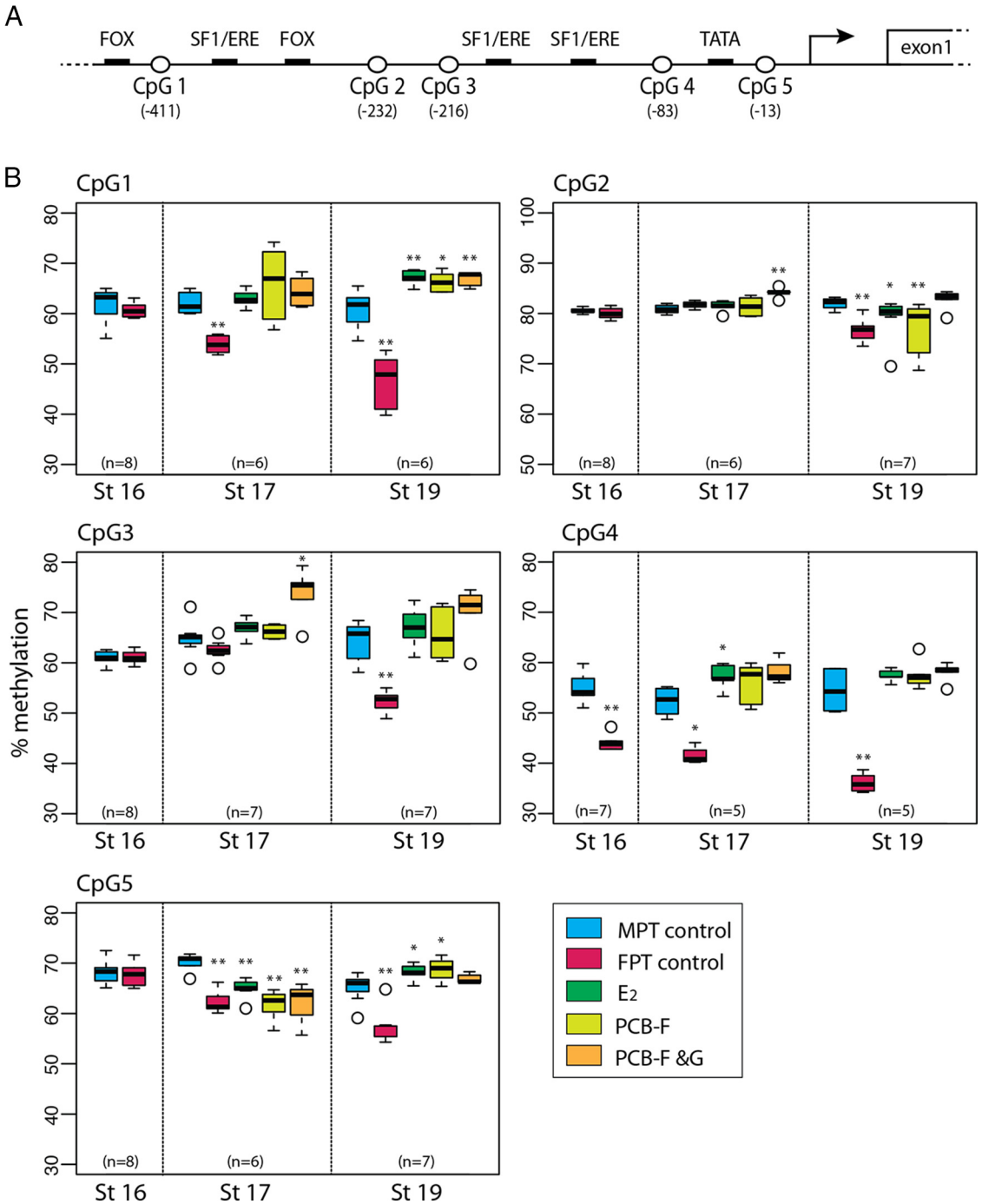

Figure 4. A percent of DNA methylation of individual CpG site in the gonadal aromatase promoter. A, CpG dinucleotide positions (CpG 1- 5) in the gonadal aromatase promoter. Putative binding sites for fork head domain factors (FOX) and vertebrate steroidogenic factor along with estrogen response element (SF1/ERE), TATA box (TATA), and transcription start site (black arrow) were previously identified in Matsumoto et al (2013). Parentheses indicate the base pair position of CpG dinucleotide relative to the transcription start site counted as +1. B, DNA methylation level at individual CpG sites (CpG 1- 5) in the gonadal aromatase promoter detected by pyrosequencing during the temperature-sensitive period. Box plot indicates interquartile range (IQR) and median. A dotted line indicates the data range with maximum 1.5 IQR. Outliers are indicated with open circles. The average number of individuals per group in each stage (n, numbers rounded up) is indicated in parenthesis. Statistical differences compared to the MPT control within a stage are indicated with asterisks (* $P < .05$, ** $P < .01$, Wilcoxon rank sum test). MPT control = EtOH vehicle at male-producing temperature. FPT control = EtOH vehicle at female-producing temperature. E_2 =10 μg 17β-estradiol treatment at MPT. PCB-F = 200 μg 4-hydroxy-2′,4′,6′-trichlorobiphenyl treatment at MPT. PCB-F&G = a mixture of 100 μg each of 4-hydroxy-2′,4′,6′-trichlorobiphenyl and 4-hydroxy-2′,3′,4′,5′-tetrachlorobiphenyl treatment at MPT. St = stage.

mechanism may be interruption of the normal MIS expression in differentiating gonads.

A previous study shows that PCB-F (4-hydroxy-2′,4′,6′-trichlorobiphenyl) has a binding affinity to the estrogen receptors that is approximately 100-fold higher than another structurally different PCB, PCB-G (4-hydroxy-2′,3′,4′,5′-tetrachlorobiphenyl) (36). In addition, PCB-F has a potent ability to achieve a maximum estrogenic activity similar to exogenous estrogens (36). Consistent with this finding, we observed that PCB-F had a stronger effect than PCB-G on gonad sex reversal against the cues of ambient temperature, and the magnitude of the effect was similar to the one induced by the exogenous estrogen, E_2 (Figure 1A, 2B). A combination of PCB-F&G treatment had a synergistic, rather than additive, effect on hatching sex ratio (Figure 1A), which is also a known characteristic of endocrine disruptors (37–40). The range of PCB concentrations examined here is comparable to the levels of PCBs found in human tissues in industrial countries (41–43).

In gonads that developed *in ovo* the overall expression pattern of gene markers followed our previous findings in response to the incubation temperatures. However the ovarian markers, *FoxL2* and *Rspo1* exhibited the expression peaks at slightly different developmental time points from the previous studies (Figure 2A compared to references 15, 16, 26). We suggest that the dissimilarity of the expression peaks is due to a different source of slider eggs (population of animals), Clark Turtle Farm and Kliebert's Turtle and Alligator Farm (both in Hammond, LA) and the fact that eggs were obtained in different years, 2006 and 2012 respectively. These egg vendors are geologically separated by approximately 1.5 miles and animals are artificially enclosed in semiwild conditions over several decades, and we can safely assume that no recent gene flow between these populations has occurred. Further, egg-laying of the red-eared slider turtles are largely influenced by environment such as climate, precipitation, time of the year, or other environmental variables. To minimize the variation attributed from different populations or natural factors, eggs from different sources or years have never been mixed within a single set of study in our laboratory. Regardless of the dissimilarity of gene expression peaks, the overall conclusion across our current and previous studies is consistent; namely that the ovarian specific markers *FoxL2* and *Rspo1* are up- or down-regulated at female- or male-producing temperature respectively.

In both PCB- and E_2-treated groups, all ovarian markers, *aromatase*, *FoxL2*, and *Rspo1* were up-regulated as expected from the hatching phenotype, but the timing of the expression was delayed compared to that observed in the FPT control (Figure 2). This transcriptional delay in response to exogenous chemicals was a stark contrast to their effect on testicular markers *Dmrt1* and *Sox9*, which instead exhibited a rapid transcriptional suppression similar to the FPT control. We presume that this temporal difference in the transcriptional responses between ovarian and testicular markers may indicate that these developmental pathways exist in a hierarchical fashion, rather than parallel manner, although understanding the true nature of this genetic cascade during gonad determination requires further investigation.

We also found that *Dmrt1* and *Sox9* exhibited a similar pattern of gene expression during gonad development (Figure 2). The close regulatory relationship between *Dmrt1* and *Sox9* has been suggested in several species. Sex-reversal of genetically female chicken by aromatase inhibitors resulted in the up-regulation of gonadal *Dmrt1* followed by an increase in *Sox9* expression (44). In adult mice, *Dmrt1* maintains *Sox9* expression in Sertoli cells; therefore, a loss of *Dmrt1* expression results in a decrease in *Sox9* expression and the loss of a testis phenotype (45). However, the interaction of *Dmrt1* and *Sox9* in gonads seems to be species-specific. In the Olive ridley sea turtle (*Lepidochelys olivacea*), *Dmrt1* expression during TSP is sexually dimorphic between the two incubation temperatures in gonads whereas *Sox9* expression is not dimorphic until the very end of TSP (46). This phenomenon appears to be consistent with many species with TSD, suggesting that *Dmrt1* may act as an upstream molecular signal during gonad determination. In mammals, the up-regulation of *Sox9* by a testis-determining gene SRY is a critical cue for the initiation of testis development. In TSD species, *Sox9* may play a different role in gonad development. The studies with TSD species show that *Sox9* is often expressed in the bipotential gonads regardless of the incubation temperature at the beginning of TSP, and down-regulated only at female-producing temperature as the development proceed. This 'down-regulation' of *Sox9* at female-specific temperature has been observed among other TSD species, including red-eared slider turtles (the current study), Olive ridley sea turtle (46, 47), and the American alligator (48).

In contrast to the rapid suppression of *Sox9* gene expression by E_2 manipulation in slider gonads (Figure 2B), the previous report by Pask and others demonstrated that *Sox9* expression does not change in E_2 treated male wallaby fetuses regardless of the up-regulation of ovarian marker, *FoxL2* (49). In this species *Sox9* is transcribed in E_2-treated gonads, but prevented from being transported into the nucleus. In our study, the effect of E_2 on factors involved in gonad determination is clearly at the transcriptional level, suggesting that E_2 reverses the gonad trajectory via species-specific mechanisms during development.

Our in vitro study showed that the gonadal expression of *FoxL2* increased just after PCB treatment; however, the effect disappeared after D20 and D12 in PCB-F and PCB-F&G treated gonad explants, respectively (Supplemental Figure 2). In contrast, the expression of *Dmrt1* was suppressed by PCB treatments in vitro throughout the observed developmental period. Overall, the response patterns of *FoxL2* and *Dmrt1* expression to PCB manipulations in vitro were similar to those observed *in ovo*, suggesting that PCB-mediated expression of candidate genes are regulated independently in the differentiating gonads.

We further studied the DNA methylation status of the aromatase promoter. Accumulating evidences suggests that DNA methylation is responsible for regulating the temperature-specific expression of the aromatase gene in TSD or TSD-related systems (19, 21, 22). Previously we identified three CpG sites (CpG 1, 4, and 5 in this study) that exhibited lower DNA methylation level at FPT than at MPT around the transcription start site of the aromatase promoter during TSP (21). In the current study we discovered two additional CpG sites (CpG 2 and 3) that were also differentially methylated between two incubation temperatures by stage 19 (Figure 4B), presumably due to a technical advantage of using the pyrosequencing method instead of a traditional sanger-sequencing. The manipulations of E_2 and PCBs at MPT did not result in demethylation of the aromatase promoter, rather the promoter maintained its normally observed methylation profiles at MPT. A similar observation is reported in chicken, where the feminization of ZZ-male was not accompanied with the full reversal of DNA methylation at the aromatase promoter (20). In sea bass, the female-biased sex ratio by exogenous estrogen application also does not accompany a change in DNA methylation pattern at the aromatase promoter (19). These studies, as well as our current study, suggest that exogenous chemicals cannot singularly reverse the epigenetic marks in differentiating gonads despite their well-established effects on transcriptional and phenotypic changes.

Several models may explain this general observation. One hypothesis is that epigenetic marks may have already been established long before gonad-specific transcription or phenotypic differentiations occurs at the beginning of TSP. Although only one, CpG 4, site exhibited a different DNA methylation pattern between MPT and FPT at stage 16, the molecular marks that are responsible for establishing the gonad-specific DNA methylation profiles may already exist before stage 16. This idea is further supported by our previous observation that the temperature-shift from FPT→MPT at stage 16 failed to establish DNA methylation patterns usually observed at constant MPT (21). Another possibility is that epigenetic marks are more stable, therefore irreversible, against environmental changes compared to other developmental processes that may be occurring during gonad differentiation. This stability may include the possibility that the steroid pathways involved in gonad differentiation investigated in this study are independent from epigenetic modifications. In summary, this study demonstrates that EDCs modify the gonadal trajectory by altering the transcriptional and phenotypic profiles, and that these elicited changes are not the consequence of an alteration in the rather stable epigenetic marks in the gonads. It supports the hypothesis that EDCs and other exogenous chemicals take an aberrant developmental pathway, rather than simply override the normal pathway set by ambient temperature, while producing nondistinguishable ovaries. Importantly, the sex determining genes examined in the current studies including aromatase are conserved across species, allowing our findings to apply beyond the mechanistic explanation in TSD system. We believe that the current study will aid in the understanding of the mechanisms underlying the interaction between environmental chemicals and gene regulation during embryonic development, that ultimately help to understand general biological problems related to endocrine disruptors in the environment that threaten human health and biodiversity of wildlife.

Acknowledgments

We acknowledge A. Buemio and M. Vafaee for technical assistance in gonad collection, A. Shindo for helpful advice on experimental procedures, and K. Kushiro for valuable suggestions on the manuscript.

Address all correspondence and requests for reprints to: David Crews, Department of Integrative Biology, University of Texas at Austin, 2415 Speedway St. Patterson labs, C0990, Austin, TX 78712, USA, Phone: +1–512–471–1804, Fax: +1–512–471–3878, Email: crews@austin.utexas.edu.

This work was supported by the National Science Foundation (grant 200701765–005 to D.C.).

Disclosure Summary: The authors have nothing to disclose.

References

1. **Harrad SJ, Sewart AP, Alcock R, Boumphrey R, Burnett V, Duarte-Davidson R, Halsall C, Sanders G, Waterhouse K, Wild SR, Jones KC.** Polychlorinated biphenyls (PCBs) in the British environment: Sinks, sources and temporal trends. *Environ Pollut*. 1994;85:131–146.
2. **Harner T, Shoeib M, Diamond M, Stern G, Rosenberg B.** Using passive air samplers to assess urban-rural trends for persistent or-

ganic pollutants. 1. Polychlorinated Biphenyls and Organochlorine Pesticides. *Environ Sci Technol*. 2004;38:4474–4483.
3. **Ross G.** The public health implications of polychlorinated biphenyls (PCBs) in the environment. *Ecotoxicol Environ Saf*. 2004;59:275–291.
4. **Jacobson JL, Humphrey HE, Jacobson SW, Schantz SL, Mullin MD, Welch R.** Determinants of polychlorinated biphenyls (PCBs), polybrominated biphenyls (PBBs), and dichlorodiphenyl trichloroethane (DDT) levels in the sera of young children. *Am J Public Health*. 1989;79:1401–1404.
5. **Bergeron JM, Klasson-Wehler E, Kuroki H.** Selective retention of hydroxylated PCB metabolites in blood. *Environ Health Perspect*. 1994;102:464–469.
6. **Hardell S, Tilander H, Welfinger-Smith G, Burger J, Carpenter DO.** Levels of polychlorinated biphenyls (PCBs) and three organochlorine pesticides in fish from the Aleutian islands of Alaska. *PLoS ONE*. 2010;5:e12396.
7. **Bergeron JM, Crews D, McLachlan JA.** PCBs as environmental estrogens: turtle sex determination as a biomarker of environmental contamination. *Environ Health Perspect*. 1994;102:780–781.
8. **Guillette LJ.** Alligators and endocrine disrupting contaminants: A Current Perspective. *Amer Zool*. 2000;40:438–452.
9. **Anway MD, Cupp AS, Uzumcu M, Skinner MK.** Epigenetic transgenerational actions of endocrine disruptors and male fertility. *Science*. 2005;308:1466–1469.
10. **Crain DA, Janssen SJ, Edwards TM, Heindel J, Ho SM, Hunt P, Iguchi T, Juul A, McLachlan JA, Schwartz J, Skakkebaek N, Soto AM, Swan S, Walker C, Woodruff TK, Woodruff TJ, Giudice LC, Guillette LJ Jr.** Female reproductive disorders: the roles of endocrine-disrupting compounds and developmental timing. *Fertil Steril*. 2008;90:911–940.
11. **Wibbels T, Crews D.** Specificity of steroid hormone-induced sex determination in a turtle. *J Endocrinol*. 1992;133:121–129.
12. **Crews D, Bergeron JM.** Role of reductase and aromatase in sex determination in the red-eared slider (Trachemys scripta), a turtle with temperature-dependent sex determination. *J Endocrinol*. 1994;143:279–289.
13. **Willingham E, Rhen T, Sakata JT, Crews D.** Embryonic treatment with xenobiotics disrupts steroid hormone profiles in hatchling red-eared slider turtles (Trachemys scripta elegans). *Environ Health Perspect*. 2000;108:329–332.
14. **Ramsey M, Crews D.** Steroid Signaling System Responds Differently to Temperature and Hormone Manipulation in the Red-Eared Slider Turtle (*Trachemys scripta elegans*), a Reptile with Temperature-Dependent Sex Determination. *Sex Dev*. 2007;1:181–196.
15. **Shoemaker C, Ramsey M, Queen J, Crews D.** Expression of Sox9, Mis, and Dmrt1 in the gonad of a species with temperature-dependent sex determination. *Dev Dyn*. 2007;236:1055–1063.
16. **Matsumoto Y, Yatsu R, Taylor C, Crews D.** Changes in gonadal gene network by exogenous ligands in temperature-dependent sex determination. *J Mol Endocrinol*. 2013;50:389–400.
17. **Pieau C, Dorizzi M.** Oestrogens and temperature-dependent sex determination in reptiles: all is in the gonads. *J Endocrinol*. 2004;181:367–377.
18. **Lance VA.** Is regulation of aromatase expression in reptiles the key to understanding temperature-dependent sex determination? *J Exp Zool A Ecol Genet Physiol*. 2009;311:312–322.
19. **Navarro-Martín L, Viñas J, Ribas L, Díaz N, Gutiérrez A, Di Croce L, Piferrer F.** DNA methylation of the gonadal aromatase (cyp19a) promoter is involved in temperature-dependent sex ratio shifts in the European sea bass. *PLoS Genet*. 2011;7:e1002447.
20. **Ellis HL, Shioda K, Rosenthal NF, Coser KR, Shioda T.** Masculine epigenetic sex marks of the CYP19A1/aromatase promoter in genetically male chicken embryonic gonads are resistant to estrogen-induced phenotypic sex conversion. *Biol Reprod*. 2012;87:23–23.
21. **Matsumoto Y, Buemio A, Chu R, Vafaee M, Crews D.** Epigenetic Control of Gonadal Aromatase (cyp19a1) in Temperature-Dependent Sex Determination of Red-Eared Slider Turtles. *PLoS ONE*. 2013;8:e63599.
22. **Parrott BB, Kohno S, Cloy-McCoy JA, Guillette LJ.** Differential incubation temperatures result in dimorphic dna methylation patterning of the SOX9 and aromatase promoters in gonads of Alligator (Alligator mississippiensis) embryos. *Biol Reprod*. 2014;90:2.
23. **Greenbaum E.** A standardized series of embryonic stages for the emydid turtle Trachemys scripta. *Can J Zool*. 2002;80:1350–1370.
24. **Crews D, Bergeron JM, McLachlan JA.** The role of estrogen in turtle sex determination and the effect of PCBs. *Environ Health Perspect*. 1995;103:73–77.
25. **Matsumoto Y, Crews D.** Molecular mechanisms of temperature-dependent sex determination in the context of ecological developmental biology. *Mol Cell Endocrinol*. 2012;354:103–110.
26. **Smith CA, Shoemaker CM, Roeszler KN, Queen J, Crews D, Sinclair AH.** Cloning and expression of R-Spondin1 in different vertebrates suggests a conserved role in ovarian development. *BMC Dev Biol*. 2008;8:72.
27. **Ramsey M, Shoemaker C, Crews D.** Gonadal expression of Sf1 and aromatase during sex determination in the red-eared slider turtle (Trachemys scripta), a reptile with temperature-dependent sex determination. *Differentiation*. 2007;75:978–991.
28. **Merchant-Larios H, Ruiz-Ramirez S, Moreno-Mendoza N, Marmolejo-Valencia A.** Correlation among thermosensitive period, estradiol response, and gonad differentiation in the sea turtle Lepidochelys olivacea. *Gen Comp Endocrinol*. 1997;107:373–385.
29. **Barske LA, Capel B.** Estrogen represses SOX9 during sex determination in the red-eared slider turtle Trachemys scripta. *Dev Biol*. 2010;341:305–314.
30. **Berg C, Holm L, Brandt I, Brunstrom B.** Anatomical and histological changes in the oviducts of Japanese quail, Coturnix japonica, after embryonic exposure to ethynyloestradiol. *Reproduction*. 2001;121:155–165.
31. **Kamata R, Takahashi S, Shimizu A, Morita M, Shiraishi F. In ovo exposure quail assay for risk assessment of endocrine disrupting chemicals.** *Arch Toxicol Springer-Verlag*. 2006;80:857–867.
32. **Picard JY, Benarous R, Guerrier D, Josso N, Kahn A.** Cloning and expression of cDNA for anti-müllerian hormone. *Proc Natl Acad Sci U S A*. 1986;83:5464–5468.
33. **Josso N, Cate RL, Picard JY, Vigier B, di Clemente N, Wilson C, Imbeaud S, Pepinsky RB, Guerrier D, Boussin L.** Anti-müllerian hormone: the Jost factor. *Recent Prog Horm Res*. 1993;48:1–59.
34. **Lee MM, Donahoe PK.** Mullerian inhibiting substance: A gonadal hormone with multiple functions. *Endocr Rev*. 1993;14:152–164.
35. **Behringer RR, Finegold MJ, Cate RL.** Müllerian-inhibiting substance function during mammalian sexual development. *Cell*. 1994;79:415–425.
36. **Carlson D, Williams D.** 4-hydroxy-2′,4′,6′-trichlorobiphenyl and 4-hydroxy-2′,3′,4′,5′- tetrachlorobiphenyl are estrogenic in rainbow trout. *Environ Toxicol Chem*. 2001;2:351–358.
37. **Arnold SF, Klotz DM, Collins BM, Vonier PM, Guillette LJ, McLachlan JA.** Synergistic Activation of Estrogen Receptor with Combinations of Environmental Chemicals. *Science*. 1996;272:1489–1492.
38. **Crews D, Putz O, Thomas P, Hayes T, Howdeshell K.** Wildlife as models for the study of how mixtures, low doses, and the embryonic environment modulate the action of endocrine-disrupting chemicals. *Pure and Applied Chemistry*. 2003;75:2305–2320.
39. **Kortenkamp A.** Ten Years of Mixing Cocktails: A Review of Combination Effects of Endocrine-Disrupting Chemicals. *Environ Health Perspect*. 2007;115:98–105.
40. **Diamanti-Kandarakis E, Bourguignon JP, Giudice LC, Hauser R, Prins GS, Soto AM, Zoeller RT, Gore AC.** Endocrine-disrupting chemicals: An Endocrine Society Scientific Statement. *Endocr Rev*. 2009;30:293–342.
41. **Chu S, Covaci A, Schepens P.** Levels and chiral signatures of per-

sistent organochlorine pollutants in human tissues from Belgium. *Environ Res*. 2003;93:167–176.
42. **Naert C, Piette M, Bruneel N, Van Peteghem C. Occurrence of polychlorinated biphenyls and polybrominated diphenyl ethers in belgian human adipose tissue samples.** *Arch Environ Contam Toxicol Springer-Verlag*. 2006;50:290–296.
43. **Schecter A, Stanley J, Boggess K, Masuda Y, Mes J, Wolff M, Fürst P, Fürst C, Wilson-Yang K, Chisholm B.** Polychlorinated biphenyl levels in the tissues of exposed and nonexposed humans. *Environ Health Perspect*. 1994;102 Suppl 1:149–158.
44. **Smith CA, Katz M, Sinclair AH.** DMRT1 is upregulated in the gonads during female-to-male sex reversal in ZW chicken embryos. *Biol Reprod*. 2003;68:560–570.
45. **Matson CK, Murphy MW, Sarver AL, Griswold MD, Bardwell VJ, Zarkower D.** DMRT1 prevents female reprogramming in the postnatal mammalian testis. *Nature*. 2011;476:101–104.
46. **Torres Maldonado LC, Landa Piedra A, Moreno Mendoza N, Marmolejo Valencia A, Meza Martı´nez A, Merchant Larios H.** Expression profiles of Dax1, Dmrt1, and Sox9 during temperature sex determination in gonads of the sea turtle Lepidochelys olivacea. *Gen Comp Endocrinol*. 2002;129:20–26.
47. **Moreno-Mendoza N, Harley VR, Merchant-Larios H.** Differential expression of SOX9 in gonads of the sea turtle Lepidochelys olivacea at male- or female-promoting temperatures. *J Exp Zool*. 1999;284:705–510.
48. **Western PS, Harry JL, Graves JA, Sinclair AH.** Temperature-dependent sex determination in the American alligator: AMH precedes SOX9 expression. *Dev Dyn*. 1999;216:411–419.
49. **Pask AJ, Calatayud NE, Shaw G, Wood WM, Renfree MB.** Oestrogen blocks the nuclear entry of SOX9 in the developing gonad of a marsupial mammal. *BMC Biol*. 2010;113.